Hindawi Publishing Corporation
Journal of Nanomaterials
Volume 2015, Article ID 670872, 6 pages
http://dx.doi.org/10.1155/2015/670872

Research Article

Influence of NH_4Cl on Hydrothermal Formation of α-$CaSO_4 \cdot 0.5H_2O$ Whiskers

Haoyuan Chen, Jing Wang, Sichao Hou, and Lan Xiang

Department of Chemical Engineering, Tsinghua University, Beijing 100084, China

Correspondence should be addressed to Lan Xiang; xianglan@mail.tsinghua.edu.cn

Received 16 November 2014; Revised 28 February 2015; Accepted 4 March 2015

Academic Editor: Yangchuan Xing

The influence of NH_4Cl on hydrothermal formation of $CaSO_4 \cdot 0.5H_2O$ whiskers from $CaSO_4 \cdot 2H_2O$ precursor at 135°C was investigated in this paper. Compared with the blank experiment, the presence of 3×10^{-2} mol·L^{-1} NH_4Cl led to the increase of the lengths of the whiskers from 50 to 160 μm to 150 to 300 μm and the decrease of the diameters from 1.0 to 1.5 μm to 0.2 to 0.5 μm. The dissolution of $CaSO_4 \cdot 2H_2O$ was accelerated by the complex interactions with NH_4Cl and the soluble cations, which led to the decrease of the induction time for the occurrence of α-$CaSO_4 \cdot 0.5H_2O$ from 46 minutes to 34 minutes and the formation of $CaSO_4 \cdot 0.5H_2O$ whiskers with high aspect ratios. Furthermore the critical supersaturation for the formation of α-$CaSO_4 \cdot 0.5H_2O$ was investigated.

1. Introduction

The formation of calcium sulfate ($CaSO_4$) whiskers with high aspect ratios has drawn much attention in recent years owing to their nontoxic and perfect mechanical properties and the wide applications in the fabrication of intensified composites [1–4]. Calcium sulfate whiskers were usually prepared by the first formation of α-$CaSO_4 \cdot 0.5H_2O$ whiskers followed by calcination at 600 to 800°C since the anisotropic –Ca–SO_4–Ca–SO_4–Ca–chains in α-$CaSO_4 \cdot 0.5H_2O$ favored their growth along *c*-axis [5].

α-$CaSO_4 \cdot 0.5H_2O$ whiskers can be prepared by wet processes, including hydrothermal method, microemulsion, or acidification methods, and the hydrothermal method has been widely used owing to its high efficiency and easy control of the formation process [6–9]. α-$CaSO_4 \cdot 0.5H_2O$ whiskers were usually produced by hydrothermal conversion of $CaSO_4 \cdot 2H_2O$ at 100 to 150°C, and the hydrothermal dissolution of $CaSO_4 \cdot 2H_2O$ and the precipitation of $CaSO_4 \cdot 0.5H_2O$ were connected with the process parameters such as the supersaturation, temperature, pH, and the organic/inorganic additives [10–15]. For example, it was reported that the presence of Sr^{2+} or PO_4^{3-} accelerated the precipitation of $CaSO_4 \cdot 2H_2O$ while the addition of Cd^{2+}, Cu^{2+}, Fe^{3+}, and Cr^{3+} inhibited the crystallization of $CaSO_4 \cdot 2H_2O$. The hydrothermal conversion of $CaSO_4 \cdot 2H_2O$ to $CaSO_4 \cdot 0.5H_2O$ was accelerated by the presence of CTAB and inhibited by the presence of arginine, aspartic acid, serine, glycine and sodium dodecyl sulfate, and so forth [16–20].

In this paper, $CaSO_4 \cdot 0.5H_2O$ whiskers with high aspect ratios were produced by hydrothermal treatment of $CaSO_4 \cdot 2H_2O$ precursor at 135°C in the presence of NH_4Cl. The influences of NH_4Cl on supersaturation, induction time, and morphology of the $CaSO_4 \cdot 0.5H_2O$ whiskers were investigated and the corresponding phenomena were discussed.

2. Experimental

2.1. Experimental Procedure. Commercial $CaSO_4 \cdot 2H_2O$ with analytical grade was sintered at 150°C for 6.0 h, then mixed with deionized water and NH_4Cl at room temperature to get the slurries containing 4.0 (wt/v) % $CaSO_4 \cdot 2H_2O$ and 0 to 7.48×10^{-2} mol·L^{-1} NH_4Cl. The slurries were then transferred to the Teflon-lined stainless autoclaves with an inner volume of 60 mL and kept under isothermal condition at 135°C for 0 to 2.0 h. After hydrothermal treatment, the products were

cooled down to 90°C naturally, filtrated, washed with alcohol for three times, and dried in air at 55°C for 12.0 h until the weight reached a stable value. The precipitates and the filtrates were collected and used for characterizations.

2.2. Characterization. The morphology of the samples were detected with the field emission scanning electron microscopy (SEM, JSM 7401F, JEOL, Japan). The average diameters and the lengths of the hydrothermal products were estimated by direct measuring about 200 particles from the typical FESEM images with magnifications of 250 to 5000. The structures of the samples were identified by powder X-ray diffractometer (XRD, D8 advanced, Brucker, Germany) using Cu Kα radiation (λ = 1.54178 Å). The solution pH was measured by a pH meter (pH meter, Mettler Toledo FE20, China).

The composition of the hydrothermal precipitates which were composed of $CaSO_4{\cdot}2H_2O$ and α-$CaSO_4{\cdot}0.5H_2O$ was detected by analyzing the contents of the crystalline water in the precipitates using differential thermal-thermogravimetric (DTA-TG) analysis (TGA/DSC1/1600HT, Mettler-Toledo, Switzerland). The soluble Ca^{2+} and $SO_4{}^{2-}$ were analyzed by EDTA titration and barium chromate spectrophotometry (Model 722, Xiaoguang, China), respectively.

3. Result and Discussion

3.1. Influence of NH_4Cl on Morphology of α-$CaSO_4{\cdot}0.5H_2O$. Figure 1 shows the effect of NH_4Cl on the XRD patterns and morphology of the hydrothermal products. XRD analyses showed that all of the hydrothermal products were composed of α-$CaSO_4{\cdot}0.5H_2O$ and most of the XRD peaks as (200), (020), and (400) were attributed to the planes parallel to *c*-axis, indicating the possible preferential growth of α-$CaSO_4{\cdot}0.5H_2O$ along the *c*-axis. The whiskers with a length of 50 to 160 μm and a diameter of 1.0 to 1.5 μm were prepared in the absence of NH_4Cl (Figure 1(a)); the increase of NH_4Cl from 7.48×10^{-3} mol·L^{-1} to 3×10^{-2} mol·L^{-1} led to the increase of the lengths from 100 to 220 μm to 150 to 300 μm, the decrease of the diameters from 0.8 to 1.2 μm to 0.2 to 0.5 μm, and the increase of the average aspect ratios from 180 to 550 (Figures 1(b) and 1(c)); in the case of 7.48×10^{-2} mol·L^{-1} NH_4Cl, the lengths and diameters of the whiskers were 160 to 330 μm and 2.2 to 4.0 μm, respectively. The presence of ethanol, potassium sodium tartrate, and sodium citrate led to the increase in the aspect ratios of $CaSO_4{\cdot}0.5H_2O$ whiskers from 1.7 to 4.8. Hou and Xiang prepared $CaSO_4{\cdot}0.5H_2O$ whiskers with average aspect ratio of 325 by hydrothermal treatment of the active $CaSO_4{\cdot}2H_2O$ precursor [10]. It is reported that the presence of ethanol and potassium sodium tartrate led to the increase in the aspect ratios of whiskers from 1.7 to 4.8 [21–23].

3.2. Influence of NH_4Cl on Composition of Precipitates and Solutions. Figure 2 shows the influence of NH_4Cl on the conversion of $CaSO_4{\cdot}2H_2O$ to α-$CaSO_4{\cdot}0.5H_2O$. α-$CaSO_4{\cdot}0.5H_2O$ occurred at about 46 minutes and converted to $CaSO_4{\cdot}0.5H_2O$ completely at about 60 minutes in the absence of NH_4Cl, while α-$CaSO_4{\cdot}0.5H_2O$ occurred at 42 minutes, 34 minutes, and 66 minutes in the presence of 7.48×10^{-3} mol·L^{-1}, 3×10^{-2} mol·L^{-1}, and 7.48×10^{-2} mol·L^{-1} NH_4Cl, respectively. The above work showed that the formation of α-$CaSO_4{\cdot}0.5H_2O$ was accelerated with the increase of NH_4Cl up to 3×10^{-2} mol·L^{-1} and then slowed down if $NH_4Cl \geq 7.48 \times 10^{-2}$ mol·L^{-1}.

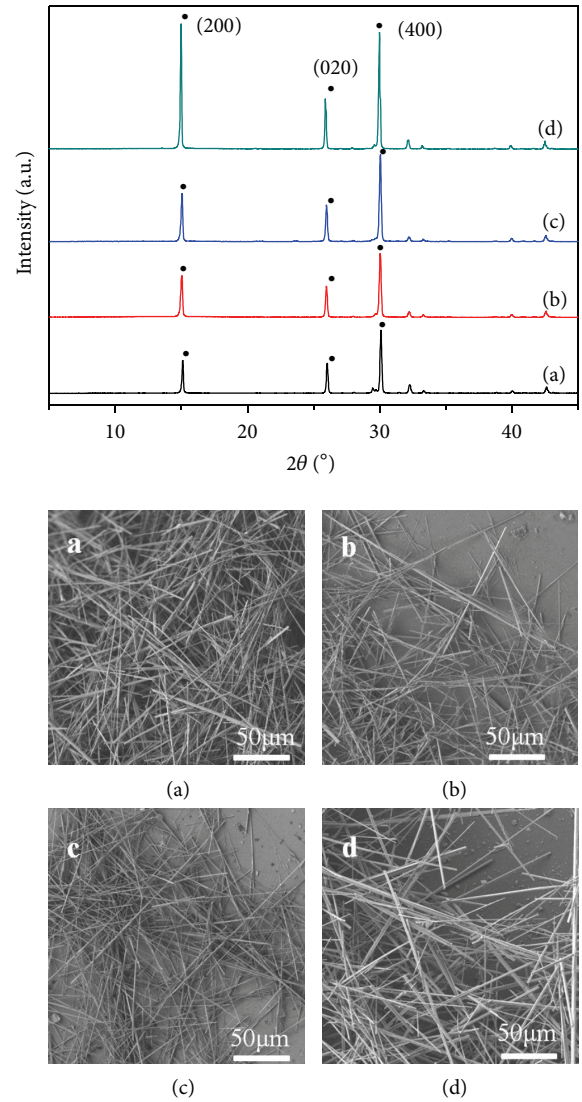

Figure 1: Influence of NH_4Cl on XRD patterns and morphology of hydrothermal products. NH_4Cl (mol·L^{-1}): a-0, b-7.48×10^{-3}, c-3×10^{-2}, d-7.48×10^{-2}; •: α-$CaSO_4{\cdot}0.5H_2O$.

Figure 3 shows the influence of NH_4Cl on pH and the concentrations of the total soluble Ca^{2+} and $SO_4{}^{2-}$ (abbreviated as $[Ca^{2+}]_T$ and $[SO_4{}^{2-}]_T$, resp.) detected in the experiments. The increase of $[Ca^{2+}]_T$ and $[SO_4{}^{2-}]_T$ and the decrease of pH with the increase of NH_4Cl should be attributed to the complex interactions of NH_4Cl and the hydrolysis of NH_4Cl, respectively. The possible reactions involved in the hydrothermal solutions at 135°C are listed in Table 1. The solubility products of $(NH_4)_2SO_4$ and $CaCl^+$ in the hydrothermal condition were $10^{0.18}$ and $10^{0.86}$, respectively, which indicated that $(NH_4)_2SO_4$ and $CaCl^+$ could

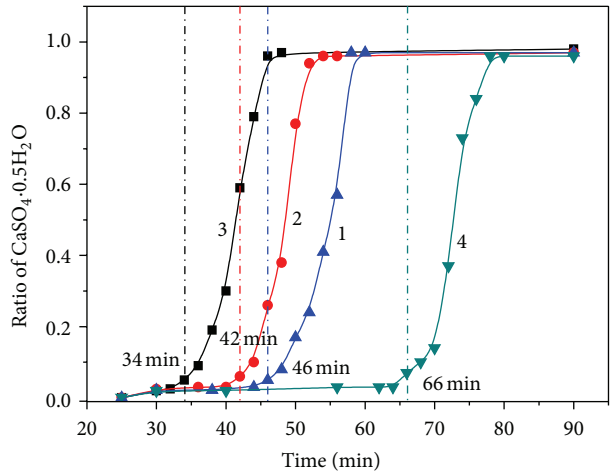

FIGURE 2: Influence of NH_4Cl on formation of $CaSO_4 \cdot 0.5H_2O$. NH_4Cl ($mol \cdot L^{-1}$): 1-0, 2-7.48×10^{-3}, 3-3×10^{-2}, 4-7.48×10^{-2}.

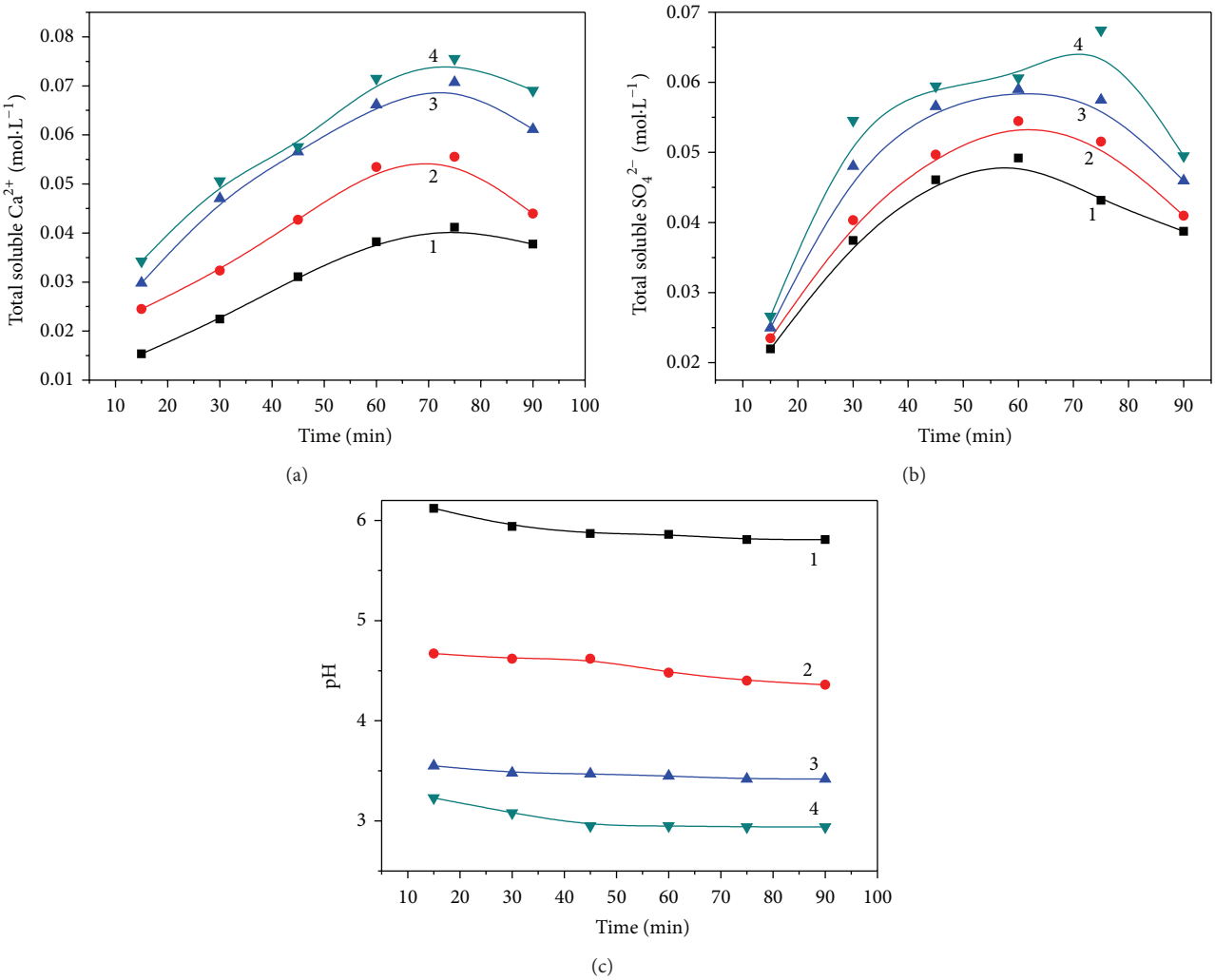

FIGURE 3: Influence of NH_4Cl on $[Ca^{2+}]_T$ (a), $[SO_4^{2-}]_T$ (b), and pH (c). NH_4Cl ($mol \cdot L^{-1}$): 1-0, 2-7.48×10^{-3}, 3-3×10^{-2}, 4-7.48×10^{-2}.

Table 1: Thermodynamic equilibrium reactions.

$NH_4^+ + Cl^- = NH_4Cl$ ($K_{sp} = 10^{-1.66}$)	$CaCl^+ + Cl^- = CaCl_2$ ($K_{sp} = 10^{-7.88}$)
$NH_4^+ + OH^- = NH_3(a) + H_2O$ ($K_{sp} = 10^{4.88}$)	$Ca^{2+} + OH^- = Ca(OH)^+$ ($K_{sp} = 10^{2.57}$)
$2NH_4^+ + SO_4^{2-} = (NH_4)_2SO_4$ ($K_{sp} = 10^{0.18}$)	$Ca(OH)^+ + OH^- = Ca(OH)_2$ ($K_{sp} = 10^{4.46}$)
$NH_4^+ + HSO_4^- = NH_4HSO_4$ ($K_{sp} = 10^{-8.66}$)	$H^+ + SO_4^{2-} = HSO_4^-$ ($K_{sp} = 10^{3.52}$)
$Ca^{2+} + Cl^- = CaCl^+$ ($K_{sp} = 10^{0.86}$)	$H^+ + HSO_4^- = H_2SO_4$ ($K_{sp} = 10^{-7.68}$)

exist stably in the hydrothermal solutions. These reactions would promote the dissolution of $CaSO_4{\cdot}2H_2O$ due to the shift of chemical equilibrium and the concentration of the total soluble Ca^{2+} (including Ca^{2+}, $CaCl^+$, $CaCl_2$, $Ca(OH)^+$, and $Ca(OH)_2$) and the total soluble SO_4^{2-} (including SO_4^{2-}, HSO_4^-, $(NH_4)_2SO_4$, NH_4HSO_4, and H_2SO_4) would increase. Similar phenomena have been reported. Jiang et al. found that the interaction between univalent NH_4^+ and SO_4^{2-} could promote the dissolution of $CaSO_4{\cdot}2H_2O$ significantly, which was called "$[MSO_4]^{(2-b)-}$ ion pair"-directed mechanism [16]. $[Ca^{2+}]_T$ and $[SO_4^{2-}]_T$ increased with the increase of the reaction time within 60 minutes, reached up to the maximum values at 60 to 75 minutes, and then decreased with further prolongation of the reaction time, revealing that the dissolution of $CaSO_4{\cdot}2H_2O$ was dominant in the initial stages and the precipitation of α-$CaSO_4{\cdot}0.5H_2O$ became gradually faster than the dissolution of $CaSO_4{\cdot}2H_2O$ in the later stages. The above phenomena confirmed the possible dissolution-precipitation mechanism for the hydrothermal formation of α-$CaSO_4{\cdot}0.5H_2O$ from $CaSO_4{\cdot}2H_2O$ precursor.

3.3. Thermodynamic Equilibrium Analysis. The equilibrium constants were calculated using reactions listed in Table 1 and the basic data in HSC chemistry 7.0 [24].

The equilibrium concentrations of the soluble species can be calculated based on the above equilibrium equations, $[Ca^{2+}]_T$, $[SO_4^{2-}]_T$, and pH detected in the experiments (Figure 3). Figure 4 shows the influence of NH_4Cl on the concentrations of free Ca^{2+}, SO_4^{2-}, and HSO_4^- (abbreviated as $[Ca^{2+}]$, $[SO_4^{2-}]$, and $[HSO_4^-]$, resp.). Free Ca^{2+} and SO_4^{2-} are the simple ion of Ca^{2+} and SO_4^{2-}, not including $CaCl^+$, $CaCl_2$, $Ca(OH)^+$, and $Ca(OH)_2$ or HSO_4^-, $(NH_4)_2SO_4$, NH_4HSO_4, and H_2SO_4. $[Ca^{2+}]$ increased with the increase of NH_4Cl (Figure 4(a)), indicating that the complex interactions among NH_4Cl and the soluble cations as Ca^{2+} accelerated the dissolution of $CaSO_4{\cdot}2H_2O$. Compared with $[Ca^{2+}]$ shown in Figure 4(a), $[SO_4^{2-}]$ was much lower and decreased with the increase of NH_4Cl (Figure 4(b)), which should be related to the hydrolysis of NH_4Cl. The hydrolysis of NH_4Cl led to the decrease of pH or the increase of $[H^+]$, which promoted the conversion of SO_4^{2-} to HSO_4^- owing to the strong complex between H^+ and SO_4^{2-}. As a result, although the total soluble SO_4^{2-} increased with the increase of NH_4Cl, the free SO_4^{2-} showed an opposite trend and decreased. In the case of the blank experiment without NH_4Cl (Figure 4(c)), $[HSO_4^-]$ was lower than 2×10^{-4} mol·L^{-1}, which was much lower than $[SO_4^{2-}]$. $[HSO_4^-]$ increased up to 5.3×10^{-2} mol·L^{-1} as the increase of $[NH_4Cl]$ up to 7.48×10^{-2} mol·L^{-1}.

3.4. Effect of Supersaturation on Induction Time. Figure 5 shows the influence of NH_4Cl on the supersaturation (S) for the formation of α-$CaSO_4{\cdot}0.5H_2O$, where $S = [[Ca^{2+}][SO_4^{2-}]/K_{sp}]$ and K_{sp} for α-$CaSO_4{\cdot}0.5H_2O$ at 135°C was $10^{-5.344}$. S increased with the increase of the reaction time up to 60–70 minutes and then decreased with further prolongation of the reaction time. S also increased with the increase of NH_4Cl up to 3×10^{-2} mol·L^{-1}, while S became quite low at 7.48×10^{-2} mol·L^{-1} NH_4Cl. The above work showed that a higher supersaturation favored the faster formation of α-$CaSO_4{\cdot}0.5H_2O$.

It was noticed that the S values at the end of the induction in solutions containing 0 to 7.48×10^{-2} mol·L^{-1} NH_4Cl were quite similar, being 209.5 (Point C), 210.2 (Point B), 208.4 (Point A), and 209.2 (Point D) at 0, 7.48×10^{-3}, 3×10^{-2}, and 7.48×10^{-2} mol·L^{-1} NH_4Cl, respectively. The points of A, B, C, and D were arranged around a horizontal line, corresponding to $S = 209.5$. Therefore, it was concluded that the critical supersaturation for the formation of α-$CaSO_4{\cdot}0.5H_2O$ at 135°C was 209.5, which was irrelevant to the presence of NH_4Cl. α-$CaSO_4{\cdot}0.5H_2O$ occurred if the solution supersaturation was higher than the critical supersaturation. S increased with the increase of NH_4Cl up to 3×10^{-2} mol·L^{-1}, which led to the decrease of the induction time for α-$CaSO_4{\cdot}0.5H_2O$. In the case of 7.48×10^{-2} mol·L^{-1} NH_4Cl, the low S led to the prolongation of the induction time for the formation of α-$CaSO_4{\cdot}0.5H_2O$ due to the hydrolysis of NH_4Cl and the decrease of $[SO_4^{2-}]$.

The morphology of α-$CaSO_4{\cdot}0.5H_2O$ was connected with the solution supersaturation. According to the traditional crystal theories, nuclei with small sizes prefer to be produced in solutions with high supersaturations, which favored the formation of $CaSO_4{\cdot}0.5H_2O$ whiskers with thin diameters and high aspect ratios. As shown in Figures 1 and 5, $CaSO_4{\cdot}0.5H_2O$ whiskers formed in the presence of 3×10^{-2} mol·L^{-1} NH_4Cl were of the smallest diameter (0.2 μm) and the highest aspect ratio (550) owing to the comparatively high S compared with those in the presence of 0, 7.48×10^{-3}, and 7.48×10^{-2} mol·L^{-1} NH_4Cl.

4. Conclusion

A facile NH_4Cl-assisted hydrothermal method was developed to synthesize α-$CaSO_4{\cdot}0.5H_2O$ whiskers with high aspect ratios. The presence of 0 to 3×10^{-2} mol·L^{-1} NH_4Cl led to the decrease of the induction period from 46 minutes to 34 minutes and the increase of the aspect ratios of the whiskers from 110 to 550. The critical supersaturation for the formation of $CaSO_4{\cdot}0.5H_2O$ was 209.5, irrelevant to the presence of NH_4Cl. In the cases of 0 to 3×10^{-2} mol·L^{-1} NH_4Cl, the complex interactions among NH_4Cl and the soluble ions led to the increase of the supersaturation, which favored the quick occurrence of α-$CaSO_4{\cdot}0.5H_2O$ nuclei with small sizes

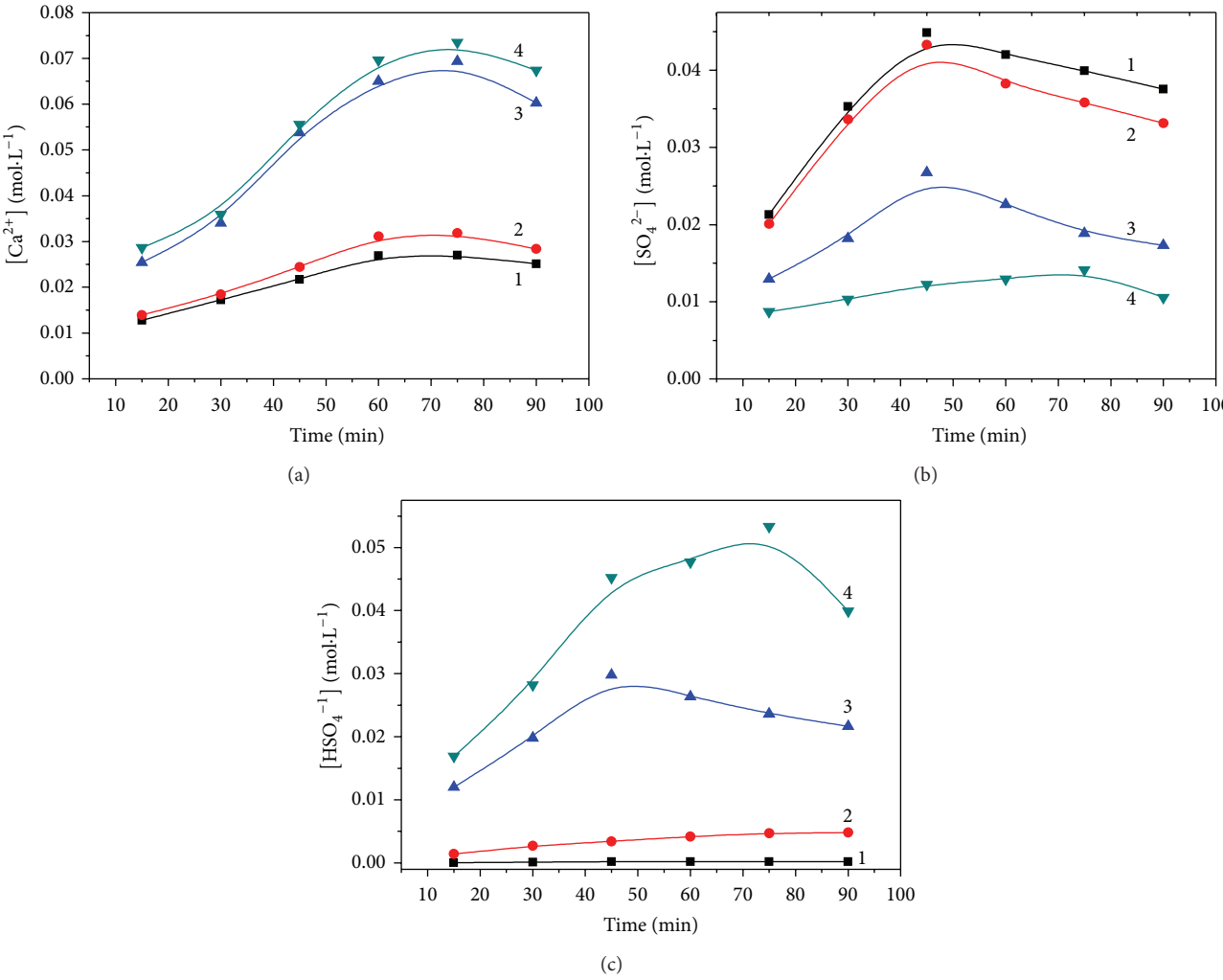

Figure 4: Influence of NH_4Cl on $[Ca^{2+}]$, $[SO_4^{2-}]$ and $[HSO_4^{-}]$. NH_4Cl (mol·L^{-1}): 1-0, 2-7.48 × 10^{-3}, 3-3 × 10^{-2}, 4-7.48 × 10^{-2}.

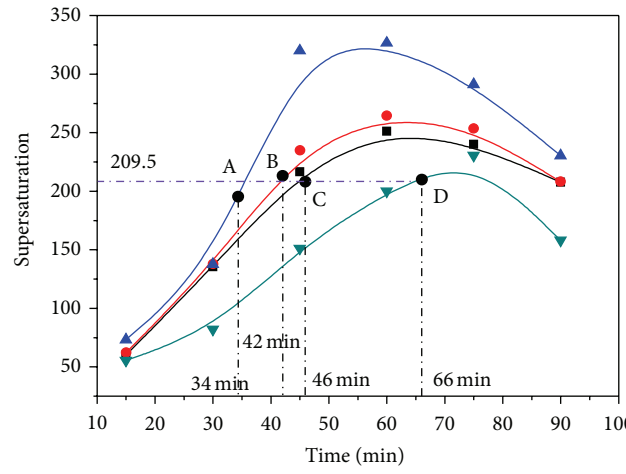

Figure 5: Influence of NH_4Cl on supersaturation. NH_4Cl (mol·L^{-1}): 1-0, 2-7.48 × 10^{-3}, 3-3 × 10^{-2}, 4-7.48 × 10^{-2}.

and promoted the formation of α-$CaSO_4 \cdot 0.5H_2O$ whiskers with high aspect ratios. In the case of 7.48×10^{-2} mol·L^{-1} NH_4Cl, the hydrolysis of NH_4Cl led to the decrease of $[SO_4^{2-}]$, which reduced the solution supersaturation and prolonged the induction period of α-$CaSO_4 \cdot 0.5H_2O$, producing α-$CaSO_4 \cdot 0.5H_2O$ with comparatively large diameters and low aspect ratios.

Conflict of Interests

The authors declare that there is no conflict of interests regarding the publication of this paper.

Acknowledgments

This project is supported by the National Science Foundation of China (nos. 51374138, 51174125, and 51234003) and the National Hi-Tech Research and Development Program of China (863 Program, 2012AA061602).

References

[1] X. F. Song, L. N. Zhang, J. C. Zhao et al., "Preparation of calcium sulfate whiskers using waste calcium chloride by reactive crystallization," *Crystal Research and Technology*, vol. 46, no. 2, pp. 166–172, 2011.

[2] R. D. Fisher, M. M. Mbogoro, M. E. Snowden et al., "Dissolution kinetics of polycrystalline calcium sulfate-based materials: influence of chemical modification," *ACS Applied Materials & Interfaces*, vol. 3, no. 9, pp. 3528–3537, 2011.

[3] T. Nissinen, M. Li, N. Brielles, and S. Mann, "Calcium sulfate hemihydrate-mediated crystallization of gypsum on Ca^{2+}-activated cellulose thin films," *CrystEngComm*, vol. 15, no. 19, pp. 3793–3798, 2013.

[4] J. Y. Liu, L. Reni, Q. Wei et al., "Fabrication and characterization of polycaprolactone/calcium sulfate whisker composites," *Express Polymer Letters*, vol. 5, no. 8, pp. 742–752, 2011.

[5] K. B. Luo, C. M. Li, L. Xiang, H. P. Li, and P. Ning, "Influence of temperature and solution composition on the formation of calcium sulfates," *Particuology*, vol. 8, no. 3, pp. 240–244, 2010.

[6] Y. Chen, Q. Wu, and Y. Ding, "Stepwise assembly of nanoparticles, -tubes, -rods, and -wires in reverse micelle systems," *European Journal of Inorganic Chemistry*, no. 31, pp. 4906–4910, 2007.

[7] W.-G. Li, L.-L. Xu, and J. Dai, "Preparation of calcium sulfate whisker from the residue of citric acid," *Journal of Synthetic Crystals*, vol. 34, no. 2, pp. 323–327, 2005.

[8] B. Guan, X. Ma, Z. Wu, L. Yang, and Z. Shen, "Crystallization routes and metastability of alpha-calcium sulfate hemihydrate in potassium chloride solutions under atmospheric pressure," *Journal of Chemical and Engineering Data*, vol. 54, no. 3, pp. 719–725, 2009.

[9] H. G. McAdie, "The effect of water vapor upon the dehydration of $CaSO_4 \cdot 2H_2O$," *Canadian Journal of Chemistry*, vol. 42, no. 4, pp. 792–801, 1964.

[10] S. C. Hou and L. Xiang, "Influence of activity of $CaSO_4 \cdot 2H_2O$ on hydrothermal formation of $CaSO_4 \cdot 0.5H_2O$ whiskers," *Journal of Nanomaterials*, vol. 2013, Article ID 237828, 5 pages, 2013.

[11] S. K. Hamdona and O. A. Al Hadad, "Influence of additives on the precipitation of gypsum in sodium chloride solutions," *Desalination*, vol. 228, no. 1–3, pp. 277–286, 2008.

[12] N. B. Singh and B. Middendorf, "Calcium sulphate hemihydrate hydration leading to gypsum crystallization," *Progress in Crystal Growth and Characterization of Materials*, vol. 53, no. 1, pp. 57–77, 2007.

[13] E. A. Abdel-Aal, M. M. Rashad, and H. El-Shall, "Crystallization of calcium sulfate dihydrate at different supersaturation ratios and different free sulfate concentrations," *Crystal Research & Technology*, vol. 39, no. 4, pp. 313–321, 2004.

[14] Y. W. Wang and F. C. Meldrum, "Additives stabilize calcium sulfate hemihydrate (bassanite) in solution," *Journal of Materials Chemistry*, vol. 22, no. 41, pp. 22055–22062, 2012.

[15] T. J. Trivedi, P. Pandya, and A. Kumar, "Effect of organic additives on the solubility behavior and morphology of calcium sulfate dihydrate (Gypsum) in the aqueous sodium chloride system and physicochemical solution properties at 35°C," *Journal of Chemical and Engineering Data*, vol. 58, no. 3, pp. 773–779, 2013.

[16] G. Jiang, H. Fu, K. Savino, J. Qian, Z. Wu, and B. Guan, "Non-lattice cation-SO_4^{2-} ion pairs in calcium sulfate hemihydrate nucleation," *Crystal Growth and Design*, vol. 13, no. 11, pp. 5128–5134, 2013.

[17] M. H. H. Mahmoud, M. M. Rashad, I. A. Ibrahim, and E. A. Abdel-Aal, "Crystal modification of calcium sulfate dihydrate in the presence of some surface-active agents," *Journal of Colloid and Interface Science*, vol. 270, no. 1, pp. 99–105, 2004.

[18] Y. Ling and G. P. Demopoulos, "Preparation of α-calcium sulfate hemihydrate by reaction of sulfuric acid with lime," *Industrial and Engineering Chemistry Research*, vol. 44, no. 4, pp. 715–724, 2005.

[19] T. Feldmann and G. P. Demopoulos, "Influence of impurities on crystallization kinetics of calcium sulfate dihydrate and hemihydrate in strong HCl-$CaCl_2$ solutions," *Industrial and Engineering Chemistry Research*, vol. 52, no. 19, pp. 6540–6549, 2013.

[20] S. K. Hamdona and U. A. Al Hadad, "Crystallization of calcium sulfate dihydrate in the presence of some metal ions," *Journal of Crystal Growth*, vol. 299, no. 1, pp. 146–151, 2007.

[21] Z. Shen, B. Guan, H. Fu, and L. Yang, "Effect of potassium sodium tartrate and sodium citrate on the preparation of α-calcium sulfate hemihydrate from flue gas desulfurization gypsum in a concentrated electrolyte solution," *Journal of the American Ceramic Society*, vol. 92, no. 12, pp. 2894–2899, 2009.

[22] Z. Pan, Y. Lou, G. Yang et al., "Preparation of calcium sulfate dihydrate and calcium sulfate hemihydrate with controllable crystal morphology by using ethanol additive," *Ceramics International*, vol. 39, no. 5, pp. 5495–5502, 2013.

[23] Z. Pan, G. Yang, Y. Lou et al., "Morphology Control and Self-Setting Modification of alpha-Calcium Sulfate Hemihydrate Bone Cement by Addition of Ethanol," *International Journal of Applied Ceramic Technology*, 2012.

[24] HSC chemistry 7.0, Outokumpu Research Oy, Pori, Finland, 2003.